

New physics in the kinematic distributions of $\bar{B} \rightarrow D^{(*)}\tau^-(\rightarrow \ell^-\bar{\nu}_\ell\nu_\tau)\bar{\nu}_\tau$

Rodrigo Alonso¹, Andrew Kobach¹ and Jorge Martin Camalich²

¹*Dept. Physics, University of California, San Diego, 9500 Gilman Drive, La Jolla, CA 92093-0319, USA*

²*PRISMA Cluster of Excellence & Institut für Kernphysik,
Johannes Gutenberg Universität Mainz, 55128 Mainz, Germany*

We investigate the experimentally-accessible kinematic distributions of the $\bar{B} \rightarrow D^{(*)}\tau^-(\rightarrow \ell^-\bar{\nu}_\ell\nu_\tau)\bar{\nu}_\tau$ decays. Specifically, we study the decay rates as functions of the $B \rightarrow D^{(*)}$ transferred squared momentum, the energy of the final charged lepton and the angle of its 3-momentum with respect to the 3-momentum of the recoiling $D^{(*)}$. The angular distribution allows to introduce new observables, like a forward-backward asymmetry, which are complementary to the total rates. We present analytic formulas for the observable 3-fold 5-body differential decay rates, study the predictions in the Standard Model and investigate the effects in different new-physics scenarios that we characterize using an effective field theory framework.

I. INTRODUCTION

The $\bar{B} \rightarrow D^{(*)}\tau^-\bar{\nu}$ decays manifest some of the most prominent anomalies in low-energy flavor observables. Significant enhancements of the rates with respect to the Standard Model (SM) predictions are observed in the two decay channels (D and D^*) and by three different experiments, BaBar [1, 2], Belle [3] and LHCb [4]. The anomalies appear in the ratios $R_{D^{(*)}} = \mathcal{B}(\bar{B} \rightarrow D^{(*)}\tau^-\bar{\nu})/\mathcal{B}(\bar{B} \rightarrow D^{(*)}\ell^-\bar{\nu})$, with $\ell = e, \mu$, where many of the experimental and theoretical uncertainties cancel.

The theoretical predictions of the $B \rightarrow D^{(*)}\tau^-\bar{\nu}$ rates in the SM are very accurate and rely on parametrizations of the form factors in an expansion about the heavy-quark limit including up to $\mathcal{O}(1/m_Q)$ corrections and constraints from unitarity [5–7]. The normalization at zero-recoil (which includes $|V_{cb}|$) and kinematic dependence of the form factors in these parametrizations are fitted to the total width and spectra of the decays into the light leptons [8]. For the decays into τ leptons the amplitude becomes sensitive to scalar form factors for which calculations in Lattice QCD (LQCD) become necessary [9–12].

The discrepancy between experiment and the SM is at the level of 4σ , and it can be explained with new physics (NP) [9, 13–30]. These analyses of the data are most fruitful when casted model-independently in an effective field theoretical framework. The results obtained in this approach can then be used as input to determine which models could explain the putative effect. In addition to $R_{D^{(*)}}$, the spectra in q^2 of the rates have also been reported by BaBar and Belle, which is useful to discriminate among the different possible NP contributions [2, 24].

However, none of the phenomenological analyses study the full kinematic distributions of the 5-body decays (or 6-body if we include the decay of the D^*), despite the fact that the experiments exploit them to extract the signal from background, mainly through Monte-Carlo simulation. Besides the dependence of the rate on q^2 and the final charged lepton energy, one can also study the dependence on the angle that the 3-momentum of this final lepton forms with the recoil direction of the $D^{(*)}$ [31–33]. The expected increase of statistics at the LHCb [4] and Belle2 [34] encourages the exploration of the discriminating power of these distributions from a theoretical point of view. Those in q^2 and E_ℓ are being used by BaBar and Belle, while the angular distribution enters indirectly in the dependence on the invariant missing mass of the decay. Casting the differential decay rate as an angular distribution offers a new method to not only discriminate among NP but also to increase the efficiency in the selection of the $\bar{B} \rightarrow D^{(*)}\tau^-\bar{\nu}$ signal events over the normalization mode, $\bar{B} \rightarrow D^{(*)}\ell^-\bar{\nu}$. In the following, we investigate the experimentally-accessible kinematic distributions of the $\bar{B} \rightarrow D^{(*)}\tau^-(\rightarrow \ell^-\bar{\nu}_\ell\nu_\tau)\bar{\nu}_\tau$ decays, in generic scenarios of NP described using an effective-field theoretical framework.

II. THE $\bar{B} \rightarrow D^{(*)}\tau^-\bar{\nu}$ DIFFERENTIAL DECAY RATES

A. The low-energy effective Lagrangian

The low-scale $O(m_b)$ effective Lagrangian for semileptonic $b \rightarrow c$ transitions is [35]:

$$\begin{aligned} \mathcal{L}_{\text{eff}} = & -\frac{G_F^{(0)}V_{cb}\eta_{\text{ew}}}{\sqrt{2}} \sum_{\ell=e,\mu,\tau} \left[\left(1 + \epsilon_L^\ell\right) \bar{\ell}\gamma_\mu(1 - \gamma_5)\nu_\ell \cdot \bar{c}\gamma^\mu(1 - \gamma_5)b + \epsilon_R^\ell \bar{\ell}\gamma_\mu(1 - \gamma_5)\nu_\ell \bar{c}\gamma^\mu(1 + \gamma_5)b \right. \\ & \left. + \bar{\ell}(1 - \gamma_5)\nu_\ell \cdot \bar{c} \left[\epsilon_S^\ell - \epsilon_P^\ell\gamma_5 \right] b + \epsilon_T^\ell \bar{\ell}\sigma_{\mu\nu}(1 - \gamma_5)\nu_\ell \cdot \bar{c}\sigma^{\mu\nu}(1 - \gamma_5)b \right] + \text{h.c.}, \end{aligned} \quad (1)$$

where we use $\sigma^{\mu\nu} = i[\gamma^\mu, \gamma^\nu]/2$, $G_F^{(0)} \equiv \sqrt{2}g^2/(8M_W^2)$ is the tree-level definition of the Fermi constant, and $\eta_{\text{ew}} = 1.006$ encodes universal short-distance electroweak corrections to the SM contribution [36] (we neglect similar corrections to the NP

contributions). The magnitude of the ϵ_i^ℓ coefficients is set by v^2/Λ^2 where Λ is the NP scale so that in the SM they vanish leaving the well-known $(V - A) \times (V - A)$ structure generated by the exchange of a W boson. The ϵ_i^ℓ coefficients can display a scale dependence (together with the corresponding hadronic matrix elements). We have assumed that potential right-handed neutrino fields (sterile with respect to the SM gauge group) are heavy compared to the low-energy scale and have been integrated out of the low-energy effective theory.¹ If the NP is coming from dynamics at $\Lambda \gg v$ and electroweak symmetry breaking is linearly realized, then an effective $SU(2)_L \times U(1)_Y$ invariant effective theory applies [35, 37]. A non-trivial consequence of this is that, at leading order in the matching between the high- and low-energy theories [23]:

$$\epsilon_R^\ell = \epsilon_R^{\ell'} + \mathcal{O}(v^4/\Lambda^4) \equiv \epsilon_R. \quad (2)$$

Therefore, any potential NP signal manifesting in ϵ_R will cancel to a large extent in the ratios $R_{D^{(*)}}$. Searches for this type of contributions can be done independently using the $\bar{B} \rightarrow D^{(*)} \ell^- \bar{\nu}_\ell$ decays [38].

B. Form factors

The hadronic matrix elements in the amplitudes derived from the effective Lagrangian in eq. (1) are parametrized in terms of form factors,

$$\langle D(k) | \bar{c} \gamma^\mu b | \bar{B}(p) \rangle = (p+k)^\mu f_+(q^2) + (p-k)^\mu f_-(q^2), \quad (3)$$

$$\langle D^*(k, \epsilon) | \bar{c} \gamma^\mu b | \bar{B}(p) \rangle = \frac{2iV(q^2)}{m_B + m_{D^*}} \varepsilon_{\mu\nu\alpha\beta} \epsilon^{*\nu} k^\alpha p^\beta, \quad (4)$$

$$\begin{aligned} \langle D^*(k, \epsilon) | \bar{c} \gamma^\mu \gamma_5 b | \bar{B}(p) \rangle &= 2m_{D^*} A_0(q^2) \frac{\epsilon^* \cdot q}{q^2} q_\mu + (m_B + m_{D^*}) A_1(q^2) \left(\epsilon_\mu^* - \frac{\epsilon^* \cdot q}{q^2} q_\mu \right) \\ &\quad - A_2(q^2) \frac{\epsilon^* \cdot q}{m_B + m_{D^*}} \left((p+k)_\mu - \frac{m_B^2 - m_{D^*}^2}{q^2} q_\mu \right), \end{aligned} \quad (5)$$

where $q = p - k$, $\varepsilon_{0123} = 1$. The $f_-(q^2)$ can be written in terms of $f_+(q^2)$ and the scalar form factor $f_0(q^2)$ using the conservation of the vector current in QCD,

$$\begin{aligned} \langle D(k) | \bar{c} b | \bar{B}(p) \rangle &= \frac{m_B^2 - m_D^2}{m_b - m_c} f_0(q^2), \\ f_0(q^2) &= f_+(q^2) + \frac{q^2}{m_B^2 - m_D^2} f_-(q^2), \end{aligned} \quad (6)$$

with $f_0(0) = f_+(0)$. The pseudoscalar form factor for the D^* channel can be related using partial conservation of the axial current:

$$\langle D^*(k, \epsilon) | \bar{c} \gamma_5 b | \bar{B}(p) \rangle = \frac{2m_{D^*}}{m_b + m_c} A_0(q^2) \epsilon^* \cdot q. \quad (7)$$

The matrix elements of the tensor operators are parameterized as:

$$\langle D(k) | \bar{c} \sigma_{\mu\nu} b | \bar{B}(p) \rangle = \frac{2if_T(q^2)}{m_B + m_D} (k_\mu p_\nu - p_\mu k_\nu), \quad (8)$$

$$\langle D^*(k, \epsilon) | \bar{c} \sigma_{\mu\nu} b | \bar{B}(p) \rangle = \frac{\epsilon^* \cdot q}{(m_B + m_{D^*})^2} T_0(q^2) \varepsilon_{\mu\nu\alpha\beta} p^\alpha k^\beta + T_1(q^2) \varepsilon_{\mu\nu\alpha\beta} p^\alpha \epsilon^{*\beta} + T_2(q^2) \varepsilon_{\mu\nu\alpha\beta} k^\alpha \epsilon^{*\beta}. \quad (9)$$

These can be related to:

$$\langle D(k) | \bar{c} \sigma_{\mu\nu} \gamma_5 b | \bar{B}(p) \rangle = \frac{2f_T(q^2)}{m_B + m_D} \varepsilon_{\mu\nu\alpha\beta} k^\alpha p^\beta, \quad (10)$$

$$\begin{aligned} \langle D^*(k, \epsilon) | \bar{c} \sigma_{\mu\nu} \gamma_5 b | \bar{B}(p) \rangle &= \frac{i\epsilon^* \cdot q}{(m_B + m_{D^*})^2} T_0(q^2) (p_\mu k_\nu - k_\mu p_\nu) + iT_1(q^2) (p_\mu \epsilon_\nu^* - \epsilon_\mu^* p_\nu) \\ &\quad + iT_2(q^2) (k_\mu \epsilon_\nu^* - \epsilon_\mu^* k_\nu), \end{aligned} \quad (11)$$

through the relation $\sigma_{\mu\nu} \gamma_5 = -i/2 \varepsilon_{\mu\nu\alpha\beta} \sigma^{\alpha\beta}$.

¹ Effective operators containing right-handed neutrinos do not interfere with the SM amplitude and therefore contribute at $\mathcal{O}(\epsilon_i^2)$ to the decay rate.

1. Numerical implementation

The q^2 -dependence of some of the form factors can be extracted experimentally analyzing the spectra of the $\bar{B} \rightarrow D^{(*)} \ell^- \bar{\nu}_\ell$ decays while a normalization factor -e.g. values of a form factor at $q^2 = q_{max}^2$ - must be calculated using nonperturbative methods in order to extract $|V_{cb}|$ from the total rates. A particularly convenient parametrization is obtained using dispersion relations in QCD and heavy-quark effective field theory (HQET) [5–7]. In this parametrization the dependence on q^2 appears through the product of the heavy-meson velocities,

$$w = v_{D^{(*)}} \cdot v_B = \frac{m_B^2 + m_{D^{(*)}}^2 - q^2}{2m_B m_{D^{(*)}}}, \quad (12)$$

where q_{max}^2 corresponds to $w_{min} = 1$, or for a variable related by a conformal mapping which optimizes the convergence of a Taylor expansion (z -expansions). In the conventional parametrization of ref. [7], the BD vector form factor is:

$$f_+(w) = \frac{V_1(w)}{r_D}, \quad V_1(w) = V_1(1) [1 - 8\rho_D^2 z + (51\rho_D^2 - 10)z^2 - (252\rho_D^2 - 84)z^3], \quad (13)$$

where $r_D = 2\sqrt{m_B m_{D^*}}/(m_B + m_{D^*})$, $z = (\sqrt{w+1} - \sqrt{2})/(\sqrt{w+1} + \sqrt{2})$ and ρ_D^2 is extracted from data. The scalar and tensor form factors are not measured and one needs to use HQET relations or LQCD. For f_0 one can use the expression derived in HQET [7, 32], but we rather implement the recent results obtained in the lattice [10–12], which are provided in terms of the z -expansion. For definiteness we use the results of the HPQCD collaboration presented in ref. [11]:

$$f_0(w) = \frac{1}{P_0} \sum_{k=0}^2 a_k^{(0)} z^k, \quad (14)$$

with $P_0 = 1 - q^2(w)/M_0^2$. For f_T there are no such calculations and we employ a relation that holds in the heavy-quark limit and at leading order in α_s :

$$f_T(w) = f_+(w) + \mathcal{O}(\Lambda/m_Q). \quad (15)$$

TABLE I: Values for the form factor parameters employed in this work. The values for $\eta_{ew}|V_{cb}|V_1(1)$, ρ_D^2 , $\eta_{ew}|V_{cb}|h_{A_1}(1)$, $\rho_{D^*}^2$, $R_1(1)$, $R_2(1)$ and their statistical correlations are obtained from the HFAG global fits to the $\bar{B} \rightarrow D^{(*)} \ell^- \bar{\nu}$ data [8]. Those for $V_1(1)$, M_0 , $a_i^{(0)}$ and their correlations are obtained from [11], $h_{A_1}(1)$ from [39] and $R_0(1)$ from ref. [13].

BD	BD^*
$\eta_{ew} V_{cb} V_1(1) = 42.65(1.53) \times 10^{-3}$	$\eta_{ew} V_{cb} h_{A_1}(1) = 35.81(0.45) \times 10^{-3}$
$\rho_D^2 = 1.185(54)$	$\rho_{D^*}^2 = 1.207(26)$
$V_1(1) = 1.035(40)$	$h_{A_1}(1) = 0.906(13)$
$M_0 = 6.420(9) \text{ GeV}$	$R_1(1) = 1.406(33)$
$a_0^{(0)} = 0.647(29)$	$R_2(1) = 0.853(20)$
$a_1^{(0)} = 0.27(30)$	$R_0(1) = 1.14(10)$
$a_2^{(0)} = -0.09(2.24)$	
$C(\eta_{ew} V_{cb} V_1(1), \rho_D^2) = 0.824$	$C(\eta_{ew} V_{cb} h_{A_1}(1), \rho_{D^*}^2) = 0.323$
$C(a_0^{(0)}, a_1^{(0)}) = -0.13$	$C(\eta_{ew} V_{cb} h_{A_1}(1), R_1(1)) = -0.108$
$C(a_0^{(0)}, a_2^{(0)}) = -0.06$	$C(\eta_{ew} V_{cb} h_{A_1}(1), R_2(1)) = -0.063$
$C(a_1^{(0)}, a_2^{(0)}) = -0.12$	$C(\rho_{D^*}^2, R_1(1)) = 0.568$
$C(a_0^{(0)}, V_1(1)) = 0.50$	$C(\rho_{D^*}^2, R_2(1)) = -0.809$
$C(a_1^{(0)}, V_1(1)) = 0.05$	$C(R_1(1), R_2(1)) = -0.758$
$C(a_2^{(0)}, V_1(1)) = 0.07$	

As for the BD^* process, the axial, vector and pseudoscalar form factors are described in terms of a HQET form factor, $h_{A_1}(w)$, and the ratios $R_i(w)$ [7, 13]:

$$\begin{aligned} V(w) &= \frac{R_1(w)}{r_{D^*}} h_{A_1}(w) & A_0(w) &= \frac{R_0(w)}{r_{D^*}} h_{A_1}(w) \\ A_1(w) &= \frac{w+1}{2} r_{D^*} h_{A_1}(w) & A_2(w) &= \frac{R_2(w)}{r_{D^*}} h_{A_1}(w), \end{aligned} \quad (16)$$

with

$$\begin{aligned}
h_{A_1}(w) &= h_{A_1}(1) [1 - 8\rho_{D^*}^2 z + (53\rho_{D^*}^2 - 15)z^2 - (231\rho_{D^*}^2 - 91)z^3], \\
R_1(w) &= R_1(1) - 0.12(w-1) + 0.05(w-1)^2, \\
R_2(w) &= R_2(1) + 0.11(w-1) - 0.06(w-1)^2, \\
R_0(w) &= R_0(1) - 0.11(w-1) + 0.01(w-1)^2.
\end{aligned} \tag{17}$$

The parameters $\rho_{D^*}^2$ and $R_{1,2}(1)$ are obtained from fits to the $\bar{B} \rightarrow D^* \ell \bar{\nu}$ spectra [8], $h_{A_1}(1)$ can be obtained from lattice calculations [39] and $R_0(1)$ can be calculated using HQET [13]. Finally, the tensor form factors can be related to $h_{A_1}(w)$ at leading order in the heavy-quark and perturbative expansions:

$$T_0(w) = \mathcal{O}(\Lambda/m_Q), \quad T_1(w) = \sqrt{m_{D^*}/m_B} h_{A_1}(w) + \mathcal{O}(\Lambda/m_Q), \quad T_2(w) = \sqrt{m_B/m_{D^*}} h_{A_1}(w) + \mathcal{O}(\Lambda/m_Q). \tag{18}$$

In Tab. I we list the numerical values for the form factor parameters and total normalizations of the amplitudes that are employed in this work. For the tensor form factors in eqs. (8, 9), we neglect the Λ/m_Q power corrections so that the sensitivity to the tensor operator in our analyses has a $\sim 25\%$ relative uncertainty. Note that combining this with the values of the HQET form factors at $w = 1$ calculated in LQCD one obtains $|V_{cb}| = 41.2(1.4)_{\text{exp}}(1.6)_{\text{th}} \times 10^{-3}$ and $|V_{cb}| = 39.5(0.5)_{\text{exp}}(0.6)_{\text{th}} \times 10^{-3}$ for $\bar{B} \rightarrow D \ell^- \bar{\nu}$ and $\bar{B} \rightarrow D^* \ell^- \bar{\nu}$ respectively.

C. The helicity amplitudes and decay rates into polarized τ

Neglecting electromagnetic radiative corrections the $B \rightarrow D^{(*)} \tau \bar{\nu}$ amplitude factorizes as:

$$\mathcal{M} = -\sqrt{2} G_F V_{cb} \{ H_V^\mu \langle \tau^- \bar{\nu} | \bar{\tau} \gamma_\mu P_L \nu | 0 \rangle + H_S \langle \tau^- \bar{\nu} | \bar{\tau} P_L \nu | 0 \rangle + H_T^{\mu\nu} \langle \tau^- \bar{\nu} | \bar{\tau} \sigma_{\mu\nu} P_L \nu | 0 \rangle \}, \tag{19}$$

with H_V^μ , H_S and $H_T^{\mu\nu}$:

$$\begin{aligned}
H_V^\mu &= (1 + \epsilon_L^\tau + \epsilon_R) \langle \bar{c} \gamma^\mu b \rangle + (\epsilon_R - \epsilon_L^\tau - 1) \langle \bar{c} \gamma^\mu \gamma_5 b \rangle, \\
H_S &= (\epsilon_{S_R}^\tau + \epsilon_{S_L}^\tau) \langle \bar{c} b \rangle + (\epsilon_{S_R}^\tau - \epsilon_{S_L}^\tau) \langle \bar{c} \gamma_5 b \rangle, \\
H_T^{\mu\nu} &= \epsilon_T^\tau \langle \bar{c} \sigma^{\mu\nu} (1 - \gamma_5) b \rangle,
\end{aligned} \tag{20}$$

subsuming Wilson coefficients and the hadronic matrix elements (schematically denoted as $\langle \dots \rangle$) of the different quark bilinears stemming from the effective Lagrangian in eq. (1). The contributions to the amplitude eq. (19) can be projected into the different angular-momentum states of the dilepton pair, characterized by its polarization vectors $\eta^\mu(\lambda)$ and using the completeness relation $g_{\mu\nu} = \sum g_{mn} \eta_\mu(m) \eta_\nu^*(n)$. The projections of H_V^μ and $H_T^{\mu\nu}$ define the helicity amplitudes,

$$H_\lambda = H_V^\mu \eta_\mu^*(\lambda), \quad H_{\lambda\lambda'} = H_T^{\mu\nu} \eta_\mu^*(\lambda) \eta_\nu^*(\lambda'). \tag{21}$$

while H_S contributes only to the $\lambda = t$ component. The tensor helicity amplitudes are antisymmetric with respect to the exchange of indices, $H_{\lambda'\lambda} = -H_{\lambda\lambda'}$.

We set the xyz coordinate system so that $\hat{z} = \vec{k}/|\vec{k}|$ in the B - or q -rest frames and with the 3-momentum of the τ , \vec{p}_τ contained in the zx plane (see Fig. 1). The kinematics of the $B \rightarrow D^{(*)} \tau \bar{\nu}$ decay can then be fully characterized by q^2 and the angle θ_τ of \vec{p}_τ relative to $-\hat{z}$ defined in the q -rest frame. The momentum and energy of the $D^{(*)}$ are functions of q^2 ; in the B -rest frame:

$$E_{D^{(*)}} = \frac{1}{2m_B} (m_B^2 + m_{D^{(*)}}^2 - q^2), \quad q^0 = \frac{1}{2m_B} (m_B^2 + q^2 - m_{D^{(*)}}^2), \quad |\vec{k}| = \frac{1}{2m_B} \sqrt{\lambda(m_B^2, m_{D^{(*)}}^2, q^2)}. \tag{22}$$

where $\lambda(x, y, z) = x^2 + y^2 + z^2 - 2(ab + ac + bc)$. For the dilepton polarization vectors we use $\eta^\mu(\pm) = (0, \pm 1, -i, 0)/\sqrt{2}$, $\eta^\mu(0) = (|\vec{k}|, 0, 0, -q^0)/\sqrt{q^2}$ and $\eta^\mu(t) = (q^0, 0, 0, -|\vec{k}|)/\sqrt{q^2}$ and for the D^* , $\epsilon^\mu(\pm) = (0, \mp 1, -i, 0)/\sqrt{2}$ and $\epsilon^\mu(0) = (|\vec{k}|, 0, 0, E_{D^*})/m_{D^*}$.

Conservation of angular momentum implies that the only non-vanishing helicity amplitudes for the $B \rightarrow D \tau \bar{\nu}$ decay are those which project into $\lambda = 0, t$ (or $\lambda + \lambda' = 0$ for the tensors):

$$\begin{aligned}
H_0 &= (1 + \epsilon_L^\tau + \epsilon_R) \frac{2m_B |\vec{k}|}{\sqrt{q^2}} f_+(q^2), \quad H_t = (1 + \epsilon_L^\tau + \epsilon_R) \frac{m_B^2 - m_D^2}{\sqrt{q^2}} f_0(q^2), \\
H_S &= (\epsilon_{S_R}^\tau + \epsilon_{S_L}^\tau) \frac{m_B^2 - m_D^2}{m_b - m_c} f_0(q^2), \quad H_{+-} = -H_{t0} = \epsilon_T^\tau \frac{2im_B |\vec{k}|}{m_B + m_D} f_T(q^2).
\end{aligned} \tag{23}$$

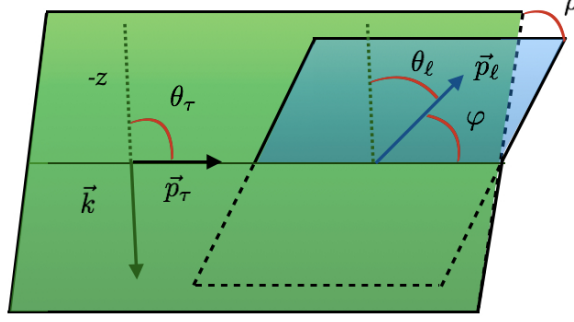


FIG. 1: Kinematics of the chain decay $\bar{B} \rightarrow D^{(*)} \tau^- (\rightarrow \ell^- \bar{\nu}_\ell \nu_\tau) \bar{\nu}_\tau$.

For the decay into polarized $D^*(\tilde{\lambda})$, conservation of angular momentum requires that the only components that contribute to the amplitude are $\lambda = \pm$ for $\tilde{\lambda} = \pm$ and $\lambda = 0, t$ for $\tilde{\lambda} = 0$ or, in case of the projections of $H_T^{\mu\nu}$, $\lambda + \lambda' = \tilde{\lambda}$. The helicity amplitudes evaluated in the B -rest frame are:

$$\begin{aligned}
H_{\pm} &= -(1 + \epsilon_L^\tau - \epsilon_R)(m_B + m_{D^*})A_1(q^2) \pm (1 + \epsilon_L^\tau + \epsilon_R) \frac{2m_B |\vec{k}|}{m_B + m_{D^*}} V(q^2), \\
H_0 &= -\frac{1 + \epsilon_L^\tau - \epsilon_R}{2m_{D^*} \sqrt{q^2}} \left[(m_B + m_{D^*}) (m_B^2 - m_{D^*}^2 - q^2) A_1(q^2) - \frac{4m_B^2 |\vec{k}|^2}{m_B + m_{D^*}} A_2(q^2) \right], \\
H_t &= -(1 + \epsilon_L^\tau - \epsilon_R) \frac{2m_B |\vec{k}|}{\sqrt{q^2}} A_0(q^2), \quad H_S = (\epsilon_{S_R} - \epsilon_{S_L}) \frac{2m_B |\vec{k}|}{m_b + m_c} A_0(q^2), \\
H_{\pm 0} &= \pm \frac{i\epsilon_T^\tau}{2\sqrt{q^2}} \left[(m_B^2 - m_{D^*}^2 \pm 2m_B |\vec{k}|)(T_1(q^2) + T_2(q^2)) + q^2(T_1(q^2) - T_2(q^2)) \right], \\
H_{\pm t} &= \frac{i\epsilon_T^\tau}{2\sqrt{q^2}} \left[(m_B^2 - m_{D^*}^2 \pm 2m_B |\vec{k}|)(T_1(q^2) + T_2(q^2)) + q^2(T_1(q^2) - T_2(q^2)) \right], \\
H_{+-} &= -H_{t0} = i\epsilon_T^\tau \left[\frac{m_B E_{D^*}}{m_{D^*}} T_1(q^2) + m_{D^*} T_2(q^2) + \frac{m_B^2 |\vec{k}|^2}{m_{D^*} (m_{D^*} + m_B)^2} T_0(q^2) \right]. \tag{24}
\end{aligned}$$

The differential decay rate for $B \rightarrow D^{(*)} \tau \bar{\nu}$ for a τ polarized along a particular direction \hat{s} is [40]:

$$d\Gamma_B(\hat{s}) = \frac{1}{2} [d\Gamma_B + (d\Gamma_B^L \hat{z}' + d\Gamma_B^\perp \hat{x}' + d\Gamma_B^T \hat{y}') \cdot \hat{s}], \tag{25}$$

where we have introduced a second coordinate system denoted by $x'y'z'$ set in the q rest-frame and defined by:

$$\hat{z}' = \frac{\vec{p}_\tau}{|\vec{p}_\tau|} = \sin \theta_\tau \hat{x} - \cos \theta_\tau \hat{z}, \quad \hat{y}' = \hat{y} = \frac{\vec{k} \times \vec{p}_\tau}{|\vec{k}| |\vec{p}_\tau|}, \quad \hat{x}' = \hat{y}' \times \hat{z}' = -\cos \theta_\tau \hat{x} - \sin \theta_\tau \hat{z}. \tag{26}$$

The different contributions to the decay rate in eq. (25) are, on one hand:

$$d\Gamma_B = d\Gamma_{B,+} + d\Gamma_{B,-}, \quad d\Gamma_B^L = d\Gamma_{B,+} - d\Gamma_{B,-}, \tag{27}$$

with the $d\Gamma_{B,\pm}$ the differential decay rates corresponding to the two helicities of the τ , $\lambda_\tau = \pm 1/2$. On the other hand, for the components orthogonal to \vec{p}_τ we have interference effects:

$$d\Gamma_B^\perp = \frac{(2\pi)^4 d\Phi_3}{2m_B} 2\text{Re} [\mathcal{M}_{B+} \mathcal{M}_{B-}^\dagger], \quad d\Gamma_B^T = \frac{(2\pi)^4 d\Phi_3}{2m_B} 2\text{Im} [\mathcal{M}_{B+} \mathcal{M}_{B-}^\dagger], \tag{28}$$

where $\mathcal{M}_{B\pm}$ is the amplitude of the $B \rightarrow D^{(*)} \tau \bar{\nu}$ decay for $\lambda_\tau = \pm 1/2$ and $d\Phi_3 \equiv d\Phi_3(p; k, p_{\bar{\nu}_\tau}, p_\tau)$ is the corresponding 3-body phase space differential element.

Solving the phase space in terms of the kinematic variables introduced above (Fig. 1) for the rates involving a given helicity of the τ leads to:

$$\begin{aligned} \frac{d^2\Gamma_{B,+}}{dq^2 d(\cos\theta_\tau)} &= \frac{G_F^2 |V_{cb}|^2 \eta_{ew}^2 |\vec{k}|}{256\pi^3 m_B^2} \left(1 - \frac{m_\tau^2}{q^2}\right)^2 \left\{ 2 \cos^2 \theta_\tau \Gamma_{0+}^0 + 2\Gamma_{0+}^t + 2 \cos \theta_\tau \Gamma_{0+}^I + \sin^2 \theta_\tau (\Gamma_{++} + \Gamma_{--}) \right\}, \\ \frac{d^2\Gamma_{B,-}}{dq^2 d(\cos\theta_\tau)} &= \frac{G_F^2 |V_{cb}|^2 \eta_{ew}^2 |\vec{k}|}{256\pi^3 m_B^2} \left(1 - \frac{m_\tau^2}{q^2}\right)^2 \left\{ 2 \sin^2 \theta_\tau \Gamma_{0-} + (1 - \cos \theta_\tau)^2 \Gamma_{+-} + (1 + \cos \theta_\tau)^2 \Gamma_{--} \right\}. \end{aligned} \quad (29)$$

where we have separated the contributions coming from the different $D^{(*)}$ and τ helicity states, $\Gamma_{\lambda,\lambda_\tau}^{(*)}$. For the decay into a $\tau(1/2)$ and a longitudinal $D^{(*)}$ we separate the three contributions stemming from the longitudinal (Γ_{0+}^0) and time-like (Γ_{0+}^t) components of the dilepton state and from their interference (Γ_{0+}^I). Note that for the BD channel all the contributions from the transversal components are equal to 0. Finally, the $\Gamma_{\lambda,\lambda_\tau}^{(X)}$ are functions of the helicity amplitudes:

$$\begin{aligned} \Gamma_{0+}^0 &= \left| 2i\sqrt{q^2} (H_{+-} + H_{0t}) - m_\tau H_0 \right|^2, & \Gamma_{0+}^t &= \left| m_\tau H_t + \sqrt{q^2} H_S \right|^2, \\ \Gamma_{0+}^I &= 2\text{Re} \left[(2i\sqrt{q^2} (H_{+-} + H_{0t}) - m_\tau H_0) (m_\tau H_t + \sqrt{q^2} H_S)^* \right], \\ \Gamma_{++} &= \left| m_\tau H_+ - 2i\sqrt{q^2} (H_{+t} + H_{+0}) \right|^2, & \Gamma_{--} &= \left| m_\tau H_- - 2i\sqrt{q^2} (H_{-t} - H_{-0}) \right|^2, \\ \Gamma_{0-} &= \left| \sqrt{q^2} H_0 - 2im_\tau (H_{+-} + H_{0t}) \right|^2, \\ \Gamma_{+-} &= \left| \sqrt{q^2} H_+ - 2im_\tau (H_{+t} + H_{+0}) \right|^2, & \Gamma_{--} &= \left| \sqrt{q^2} H_- - 2im_\tau (H_{-t} - H_{-0}) \right|^2. \end{aligned} \quad (30)$$

Likewise, the contribution to the rate of the interference term $d\mathcal{L}_B \equiv (2\pi)^4 d\Phi_3 / (2m_B) \mathcal{M}_{B+} \mathcal{M}_{B-}^\dagger$ is:

$$\frac{d^2\mathcal{L}_B}{dq^2 d(\cos\theta_\tau)} = \frac{G_F^2 |V_{cb}|^2 \eta_{ew}^2 |\vec{k}|}{256\pi^3 m_B^2} \left(1 - \frac{m_\tau^2}{q^2}\right)^2 \sin\theta_\tau \left[2\mathcal{I}_0 \cos\theta_\tau + 2\mathcal{I}_0^I + \mathcal{I}_+(1 - \cos\theta_\tau) + \mathcal{I}_-(1 + \cos\theta_\tau) \right], \quad (31)$$

where

$$\begin{aligned} \mathcal{I}_0 &= m_\tau \sqrt{q^2} |H_0|^2 + 4m_\tau \sqrt{q^2} |H_{+-} + H_{0t}|^2 + 2im_\tau^2 H_0 (H_{+-} + H_{0t})^* - 2iq^2 H_0^* (H_{+-} + H_{0t}), \\ \mathcal{I}_0^I &= -\sqrt{q^2} H_0^* (m_\tau H_t + \sqrt{q^2} H_S) - 2im_\tau (H_{+-} + H_{0t})^* (m_\tau H_t + \sqrt{q^2} H_S), \\ \mathcal{I}_+ &= m_\tau \sqrt{q^2} |H_+|^2 + 2im_\tau^2 H_+ (H_{+t} + H_{+0})^* - 2iq^2 H_+^* (H_{+t} + H_{+0}) + 4m_\tau \sqrt{q^2} |H_{+t} + H_{+0}|^2, \\ \mathcal{I}_- &= -m_\tau \sqrt{q^2} |H_-|^2 - 2im_\tau^2 H_- (H_{-t} - H_{-0})^* + 2iq^2 H_-^* (H_{-t} - H_{-0}) - 4m_\tau \sqrt{q^2} |H_{-t} - H_{-0}|^2. \end{aligned} \quad (32)$$

The differential forms for the $\Gamma_B^{\perp,T}$ observables are obtained taking twice the real or imaginary part in eq. (31). Note that the latter observable is a triple-product correlation that, in the absence of final-state interactions, is T -odd and becomes sensitive to NP sources of CP -violation entering in the process through the Wilson coefficients [40].

III. THE $\bar{B} \rightarrow D^{(*)}\tau^- (\rightarrow \ell^- \bar{\nu}_\ell \nu_\tau) \bar{\nu}_\tau$ DECAY RATE

A. The leptonic τ decay

In the SM, the differential decay rate $\tau^- \rightarrow \ell^- \bar{\nu}_\ell \nu_\tau$ with the τ lepton with helicity λ_τ is:

$$d\Gamma_{\tau,\lambda_\tau} = \frac{32G_F^2 (2\pi)^4}{m_\tau} (p_{\nu_\tau} \cdot p_\ell) [p_{\bar{\nu}_\ell} \cdot (p_\tau - m_\tau s_{\lambda_\tau})] \delta^{(4)}(p_\tau - p_\ell - p_{\bar{\nu}_\ell} - p_{\nu_\tau}) \frac{d^3\vec{p}_\ell}{2E_\ell (2\pi)^3} \frac{d^3\vec{p}_{\bar{\nu}_\ell}}{2E_{\bar{\nu}_\ell} (2\pi)^3} \frac{d^3\vec{p}_{\nu_\tau}}{2E_{\nu_\tau} (2\pi)^3}, \quad (33)$$

where s_{λ_τ} is the spin 4-vector of the τ . Integrating over the phase space of the neutrinos,

$$\int \frac{d^3\vec{p}_{\bar{\nu}_\ell}}{2E_{\bar{\nu}_\ell} (2\pi)^3} \frac{d^3\vec{p}_{\nu_\tau}}{2E_{\nu_\tau} (2\pi)^3} p_{\bar{\nu}_\ell}^\alpha p_{\nu_\tau}^\beta \delta^{(4)}(p_\tau - p_\ell - p_{\bar{\nu}_\ell} - p_{\nu_\tau}) = \frac{1}{48(2\pi)^5} \left[(p_\tau - p_\ell)^2 g^{\alpha\beta} + 2(p_\tau - p_\ell)^\alpha (p_\tau - p_\ell)^\beta \right], \quad (34)$$

one obtains,

$$d\Gamma_{\tau,\lambda_\tau} = \frac{G_F^2}{3(2\pi)^4} \frac{d^3\vec{p}_\ell}{m_\tau E_\ell} p_{\ell,\alpha} (p_\tau - m_\tau s_{\lambda_\tau})_\beta [(p_\tau - p_\ell)^2 g^{\alpha\beta} + 2(p_\tau - p_\ell)^\alpha (p_\tau - p_\ell)^\beta]. \quad (35)$$

For the sake of simplicity, we will assume in the following that $m_\ell = 0$, which should hold with good accuracy for most of the kinematics of the decays considered in this work.

To resolve the τ decay in $\bar{B} \rightarrow D^{(*)}\tau^- (\rightarrow \ell^- \bar{\nu}_\ell \nu_\tau) \bar{\nu}_\tau$, it is convenient to use the coordinate system $x'y'z'$ introduced above. The spherical coordinates of \vec{p}_ℓ in this basis are the polar angle φ with respect to \hat{z}' , and the corresponding azimuthal angle ρ with respect to the $x'z'$ plane (see Fig. 1). In this coordinate system, using eq. (35) in the q rest-frame, we obtain:

$$\frac{d\Gamma_{\tau,\pm}}{dE_\ell d(\cos\varphi) d\rho} = \frac{G_F^2}{3(2\pi)^4} \frac{E_\ell^2}{m_\tau} [(E_\tau - |\vec{p}_\tau| \cos\varphi)(3m_\tau^2 - 4E_\ell(E_\tau - |\vec{p}_\tau| \cos\varphi)) \pm (E_\tau \cos\varphi - |\vec{p}_\tau|)(m_\tau^2 - 4E_\ell(E_\tau - |\vec{p}_\tau| \cos\varphi))], \quad (36)$$

where $E_\tau = (q^2 + m_\tau^2)/(2\sqrt{q^2})$ and $|\vec{p}_\tau| = (q^2 - m_\tau^2)/(2\sqrt{q^2})$. Integrating in all the phase space and averaging over polarizations we find that the branching fraction of the $\tau^- \rightarrow \ell^- \bar{\nu}_\tau \nu_\ell$ decay is:

$$\mathcal{B}[\tau_\ell] = \tau_\tau \frac{G_F^2 m_\tau^5}{192\pi^3}, \quad (37)$$

where τ_τ is the τ -lepton lifetime $\tau_\tau = 1/\Gamma_\tau$. This expression leads, numerically, to $\mathcal{B}[\tau_\ell] = 0.178$ which, at the level of precision of this study, is well in agreement with the experimental data [41].

Like in the case of the B decay, one may also study the decays rates for τ with the spin pointing to an arbitrary direction. This will involve, in general, interference effects between the τ helicity decay amplitudes, $\mathcal{M}_{\tau\pm}$. Defining the contribution of these terms to the rate as $d\mathcal{I}_\tau \equiv (2\pi)^4 d\Phi_3(p_\tau; p_\ell, p_{\bar{\nu}_\ell})/(2m_B)\mathcal{M}_{\tau+}\mathcal{M}_{\tau-}^\dagger$, one obtains:

$$\frac{d^3\mathcal{I}_\tau}{dE_\ell d(\cos\varphi) d\rho} = \frac{G_F^2}{3(2\pi)^4} E_\ell^2 [e^{i\rho} \sin\varphi (m_\tau^2 - 4E_\ell(E_\tau - |\vec{p}_\tau| \cos\varphi))]. \quad (38)$$

B. The 5-body differential decay rate

The $\bar{B} \rightarrow D^{(*)}\tau^- (\rightarrow \ell^- \bar{\nu}_\ell \nu_\tau) \bar{\nu}_\tau$ decay amplitude is:

$$\mathcal{M} = \frac{4G_F^2 V_{cb} \eta_{ew}}{p_\tau^2 - m_\tau^2 + i m_\tau \Gamma_\tau} \sum_{\lambda_\tau = \pm 1/2} \langle \ell^- \bar{\nu}_\ell | \bar{\ell} \gamma^\rho P_L \nu_\ell | 0 \rangle \langle \nu_\tau | \bar{\nu}_\tau \gamma_\rho P_L \tau | \tau^-(\lambda_\tau) \rangle \times \\ \times \{ H_V^\mu \langle \tau^-(\lambda_\tau) \bar{\nu}_\tau | \bar{\tau} \gamma_\mu P_L \nu_\tau | 0 \rangle + H_S \langle \tau^-(\lambda_\tau) \bar{\nu}_\tau | \bar{\tau} P_L \nu_\tau | 0 \rangle + H_T^{\mu\nu} \langle \tau^-(\lambda_\tau) \bar{\nu}_\tau | \bar{\tau} \sigma_{\mu\nu} P_L \nu_\tau | 0 \rangle \}, \quad (39)$$

where we have used the completeness relation $\not{p}_\tau + m_\tau = \sum_{\lambda_\tau} u(p_\tau, \lambda_\tau) \bar{u}(p_\tau, \lambda_\tau)$ and the amplitude factorizes into the $\bar{B} \rightarrow D^{(*)}\tau^-(\lambda_\tau) \bar{\nu}_\tau$ and $\tau^-(\lambda_\tau) \rightarrow \ell^- \bar{\nu}_\ell \nu_\tau$ amplitudes. The phase space differential volume of the 5-body decay also factorizes into those of the two 3-body decays according to the formula:

$$d\Phi_5(p; k, p_{\bar{\nu}_\tau}, p_\ell, p_{\bar{\nu}_\ell}, p_{\nu_\tau}) = (2\pi)^3 d\Phi_3(p; k, p_{\bar{\nu}_\tau}, p_\tau) d\Phi_3(p_\tau; p_\ell, p_{\bar{\nu}_\ell}, p_{\nu_\tau}) dp_\tau^2. \quad (40)$$

In the narrow-width approximation, $\Gamma_\tau \ll m_\tau$, which applies to an excellent degree here:

$$\frac{1}{(p_\tau^2 - m_\tau^2)^2 + m_\tau^2 \Gamma_\tau^2} \xrightarrow{\Gamma_\tau \ll m_\tau} \frac{\pi}{m_\tau \Gamma_\tau} \delta(p_\tau^2 - m_\tau^2), \quad (41)$$

the τ is on-shell, resolving the phase-space integral in dp_τ^2 . Combining eqs. (39, 40, 41) we arrive at:

$$d\Gamma = \tau_\tau \sum_{\lambda_\tau = \pm 1/2} d\Gamma_{B,\lambda_\tau} \times d\Gamma_{\tau,\lambda_\tau} + \tau_\tau d\mathcal{I}_B \times d\mathcal{I}_\tau + \text{c.c.} \quad (42)$$

$$= \tau_\tau \sum_{\lambda_\tau = \pm 1/2} d\Gamma_{B,\lambda_\tau} \times d\Gamma_{\tau,\lambda_\tau} + \tau_\tau (\cos\rho d\Gamma_B^\perp - \sin\rho d\Gamma_B^T) d|\mathcal{I}_\tau|. \quad (43)$$

where, in the second line, we have used eq. (38) and introduced the polarization observables in eq. (25). The 5-body differential decay rate $d\Gamma$ is a function of q^2 , E_ℓ and the angular variables ρ , $\cos\theta_\ell$ and $\cos\varphi$ introduced above and shown in Fig. 1. It is relevant to point out that ρ is the only variable in the expression above linking the production and decay systems. In particular it introduces a correlation between the production $D^{(*)}-\tau$ plane and the decay $\tau-\ell$ plane. One can also see from Eq. (43) that after integration in $\rho \in (-\pi, \pi)$ the interference term vanishes and the intuitive implementation of the narrow width approximation holds [42]. Nevertheless, since the present work will discuss angular distributions the interference term does have an effect.

1. Integrating the τ angular phase-space

Experiments can, at best, measure the distribution of decays with respect to the variables q^2 , E_ℓ and the angle of the 3-momentum of this final-state lepton relative to the one of the $D^{(*)}$, that we define analogously to θ_τ , in the q rest frame, as:

$$\cos \theta_\ell = -\frac{\vec{p}_\ell \cdot \vec{k}}{|\vec{p}_\ell| |\vec{k}|} = -\frac{\vec{p}_\ell \cdot \hat{z}}{|\vec{p}_\ell|} = \cos \theta_\tau \cos \varphi + \sin \theta_\tau \sin \varphi \cos \rho, \quad (44)$$

We now need to integrate the expression of the 5-body differential decay rate in eq. (43) only in the angular phase space of the τ . To do this, we use eq. (44) to transform the angular variables:

$$(\rho, \cos \theta_\tau, \cos \varphi) \rightarrow (\cos \theta_\ell, \cos \theta_\tau, \cos \varphi), \quad (45)$$

and we integrate in $\cos \theta_\tau$ and in $\cos \varphi$ for a given $\cos \theta_\ell$. Before we proceed, note that this transformation maps the domain of integration Θ defined by $\rho \in [-\pi, 0] \cup [0, \pi]$ and $\cos \theta_\tau \in [-1, 1]$ twice onto Θ' delimited by $\cos \theta_\ell \in [-1, 1]$ and $\cos \theta_\tau^\pm = \cos(\theta_\ell \mp \varphi)$. The contribution to the decay rate from any differential of phase space in Θ' is then related to the sum of the corresponding ones in Θ , which are themselves related by $d\rho f(\rho)|_{[-\pi, 0]} = d\rho f(-\rho)|_{[0, \pi]}$ and where, as shown in eq. (43), $f(\rho)$ can be 1, $\cos \rho$ or $\sin \rho$. Therefore, the contributions from decay rates without interference $d\Gamma_{B, \lambda_\tau} \times d\Gamma_{\tau, \lambda_\tau}$ and from $d\Gamma_B^\perp$ should be multiplied by a factor 2 when integrating over Θ' . On the other hand, the *contribution of the CP-odd observable $d\Gamma_B^\perp$ vanishes from the angular distribution in $\cos \theta_\ell$* . This can be understood noticing that the relative $D^{(*)} - \tau$ angle is the same for ρ and $-\rho$, whereas the CP odd contribution changes sign.

TABLE II: Results for all the nonvanishing angular integrals $I_f(\theta_\ell, \varphi)$ defined in eq. (46).

$f(\theta_\tau)$	1	$\cos \theta_\tau$	$\cos^2 \theta_\tau$	$\cos \rho \sin \theta_\tau$	$\cos \rho \sin(2\theta_\tau)$
$I_f(\theta_\ell, \varphi)$	π	$\pi \cos \theta_\ell \cos \varphi$	$\pi (\cos^2 \theta_\ell \cos^2 \varphi + \frac{1}{2} \sin^2 \theta_\ell \sin^2 \varphi)$	$\pi \cos \theta_\ell \sin \varphi$	$\pi \sin \varphi \cos \varphi (3 \cos^2 \theta_\ell - 1)$

Now we turn to the integration on θ_τ . These integrals are of the form:

$$I_f(\theta_\ell, \varphi) = \int_{\cos \theta_\tau^-}^{\cos \theta_\tau^+} d(\cos \theta_\tau) |\det \mathbf{J}| f(\theta_\tau), \quad (46)$$

where $f(\theta_\tau)$ is a given function and $\det \mathbf{J}$ is the determinant of the Jacobian of the transformation in eq. (45):

$$\det \mathbf{J} = -\frac{1}{\sin \rho \sin \theta_\tau \sin \varphi} = -(1 - \cos^2 \theta_\tau - \cos^2 \varphi - \cos^2 \theta_\ell + 2 \cos \theta_\tau \cos \varphi \cos \theta_\ell)^{-1/2}, \quad (47)$$

The dependence of the rate in θ_τ enters through the Jacobian or through $f(\theta_\tau)$, which encompasses the angular dependence of the $B \rightarrow D^{(*)} \tau^- \bar{\nu}_\tau$ rates, eqs. (29, 31) or of $\cos \rho$ via eq. (44) in case of the interference term in eq. (43).² In Tab. II we collect the results for the different (nonvanishing) integrals that appear. In consistency with the discussion above regarding the contribution of the interference term $d\Gamma_B^\perp$ to the rate, the last two columns vanish when integrated over the full range of $\cos \theta_\ell$.

The integral in the angular variable $\cos \varphi$ is also subtle. The energy of the final charged-lepton in the τ rest frame, \tilde{E}_ℓ and the one in the q rest-frame are related by the boost:

$$\tilde{E}_\ell = \gamma(E_\ell - \beta \cos \varphi), \quad (48)$$

where $\gamma = E_\tau/m_\tau$ and $\gamma\beta = |\vec{p}_\tau|/m_\tau$. Thus, this integral involves non-flat boundaries in the phase-space variables E_ℓ and φ that account for the fact that some energy configurations in the q -rest frame can only be reached for certain polar angles φ , e.g. the maximum possible energy for the lepton, $E_\ell^{\max} = \sqrt{q^2}/2$, can only be reached when it is aligned with the τ momenta so that the relativistic γ factor is the largest. More generally, there are two regions of integration:

$$E_\ell \in \left[\frac{m_\tau^2}{2\sqrt{q^2}}, \frac{\sqrt{q^2}}{2} \right], \quad \cos \varphi \in \left[\frac{1}{\beta} - \frac{m_\tau}{2\gamma\beta E_\ell}, 1 \right]. \quad (49)$$

² Note that this is one of the benefits of the q rest frame; in a different frame E_τ in eq. (36) depends on θ_τ . the results for all the integrals appearing in our case.

where for every E_ℓ there is only an angle with respect to the boost direction \hat{z}' , over which we integrate. The second is the region,

$$E_\ell \in \left[0, \frac{m_\tau^2}{2\sqrt{q^2}}\right], \quad \cos \varphi \in [-1, 1], \quad (50)$$

that covers the maximum energies that can be reached by all the polar angles φ .

We can now write the experimentally accessible 3-fold 5-body differential decay rate as:

$$\frac{d^3\Gamma_5}{dq^2 dE_\ell d(\cos \theta_\ell)} = \mathcal{B}[\tau_\ell] \frac{G_F^2 |V_{cb}|^2 \eta_{ew}^2 |\vec{k}|}{32\pi^3 m_B^2} \left(1 - \frac{m_\tau^2}{q^2}\right)^2 \frac{E_\ell^2}{m_\tau^3} \times [I_0(q^2, E_\ell) + I_1(q^2, E_\ell) \cos \theta_\ell + I_2(q^2, E_\ell) \cos^2 \theta_\ell], \quad (51)$$

where the different angular coefficients are functions of q^2 and E_ℓ . The angle θ_ℓ is in the interval $[0, \pi]$, whereas for q^2 and E_ℓ we have two distinct regions of phase space corresponding to the two regions of integration above. Given q^2 in the interval $[m_\tau^2, (m_B - m_{D^{(*)}})^2]$, the decay rate as a function of E_ℓ is defined piecewise over two different domains: one is the region of phase space where $E_\ell \in [m_\tau^2/(2\sqrt{q^2}), \sqrt{q^2}/2]$, that we call ω_1 , and the second one corresponds to $E_\ell \in [0, m_\tau^2/(2\sqrt{q^2})]$ or ω_2 . We plot these regions and show the resulting expressions for the $I_i(q^2, E_\ell)$ in the Appendix A.

The angular coefficients in eq. (51) are new observables that are complementary to the total rates. For instance, the angle can be integrated:

$$\frac{d^2\Gamma_5}{dq^2 dE_\ell} = \mathcal{B}[\tau_\ell] \frac{G_F^2 |V_{cb}|^2 \eta_{ew}^2 |\vec{k}|}{16\pi^3 m_B^2} \left(1 - \frac{m_\tau^2}{q^2}\right)^2 \frac{E_\ell^2}{m_\tau^3} \times \left[I_0(q^2, E_\ell) + \frac{1}{3}I_2(q^2, E_\ell)\right], \quad (52)$$

showing that the total rates only depend on the functions $I_{0,2}(q^2, E_\ell)$. This implies that we would obtain a completely independent observable by measuring the coefficient $I_1(q^2, E_\ell)$, which could be done defining a forward-backward asymmetry with respect to the angle θ_ℓ :

$$\frac{d^2 A_{FB}(q^2, E_\ell)}{dq^2 dE_\ell} = \left(\int_0^1 d(\cos \theta_\ell) - \int_{-1}^0 d(\cos \theta_\ell)\right) \frac{d^3\Gamma_5}{dq^2 dE_\ell d(\cos \theta_\ell)}. \quad (53)$$

An interesting integrated observable that could be constructed using this forward-backward asymmetry is:

$$R_{FB}^{(*)} = \frac{1}{\mathcal{B}[\tau_\ell]} \frac{1}{\Gamma_{\text{norm.}}} A_{FB}, \quad (54)$$

which is labeled according to whether it corresponds the BD (R_{FB}) or BD^* (R_{FB}^*) channel. In these definitions we have normalized with the total rate of the normalization decay $B \rightarrow D^{(*)} \ell \bar{\nu}_\ell$, $\Gamma_{\text{norm.}}$, and the branching fraction of the leptonic τ -decay. The third element in eq. (54), A_{FB} , is the integrated observable in eq. (53) that could be obtained experimentally subtracting the number of total events in the backward and forward directions.

IV. PHENOMENOLOGY

In Fig. 2 we show the q^2 -spectrum of the the total rates and the forward-backward asymmetries normalized as branching-fractions and where we have factored out the $\mathcal{B}[\tau_\ell]$. The observables of the BD and BD^* modes are labeled as the $\Gamma(A_{FB})$ and $\Gamma^*(A_{FB}^*)$, respectively. The uncertainties in the SM predictions correspond to the 1σ intervals assuming (correlated) Gaussian distributions for the inputs listed in Tab. I. Along with these predictions we show the results in three different benchmark scenarios of NP. In the first NP scenario, denoted as ‘‘Current’’ we only consider a modification of the normalization of the decay via $\epsilon_L^\tau = 0.15$. In the ‘‘Scalar’’ scenario we set all $\epsilon_i = 0$ except for $\epsilon_{S_L}^\tau = 0.80$ and $\epsilon_{S_R}^\tau = -0.65$, while in the ‘‘Tensor’’ one we only allow for $\epsilon_T^\tau = 0.40$. Scenarios of this type could explain the $R_{D^{(*)}}$ anomalies with NP at a scale of $\Lambda \sim 1$ TeV, as discussed in refs. [9, 16, 17, 19, 21–24].

These plots show the different dependencies of the observables on the NP scenarios considered here which lead to results unambiguously distinct from the SM, even accounting for the theoretical uncertainties. Hence, a measurement of the angular observables with enough precision could help to confirm and eventually identify the contribution responsible for the enhancements measured in $R_{D^{(*)}}$. The $A_{FB}^{(*)}$ present a mild dependence on the scalar and current interactions which is not very different from the one of $R_{D^{(*)}}$. On the other hand, the asymmetries are very sensitive to the tensor interactions, especially for the BD^*

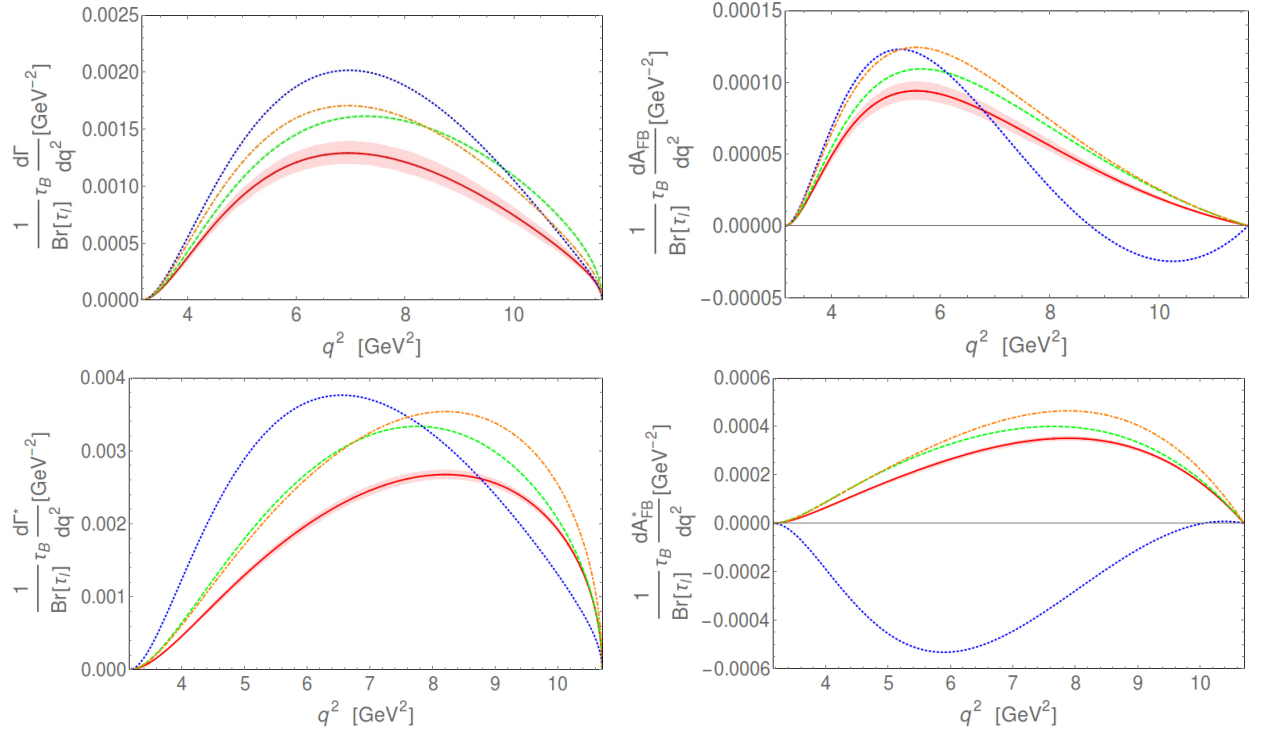


FIG. 2: Decay rates and forward-backward asymmetries, as defined in eq. (53), normalized as B^\pm life-time and factoring out the branching fraction of the leptonic τ decay. Along with the SM prediction plotted in solid red, we show the results in the three benchmark scenarios of NP (see main text): “Current” as the dot-dashed (orange) curve, “Scalar” as the dashed (green) curve and “Tensor” as the dotted (blue) one. The uncertainties of the SM predictions correspond to the 1σ intervals assuming (correlated) Gaussian distributions for the inputs listed in Tab. I

TABLE III: Numerical results on the observables $R_{D^{(*)}}$ and R_{FB}^* in the SM and in the different benchmark scenarios of NP (see main text) obtained using the inputs listed in Tab. I. The experimental averages are taken from ref. [8].

	R_D	R_{FB}	R_{D^*}	R_{FB}^*
SM	0.310(19)	0.0183(9)	0.252(4)	0.0310(7)
Current	0.410	0.0242	0.333	0.0410
Scalar	0.400	0.0218	0.315	0.0363
Tensor	0.467	0.0151	0.346	-0.0377
Expt.	0.391(41)(28)	-	0.322(18)(12)	-

channel where A_{FB}^* changes sign for the values of ϵ_T^τ considered here. In Tab. III we present the corresponding predictions for the integrated observables R_{FB}^* defined in eq. (54), which manifest similar patterns to those in Fig. 2.

An important feature of our results concerns the absolute value of the contribution of the forward-backward asymmetries to the differential decay rate. Indeed, as shown in Fig. 2 and Tab. III, the contributions of A_{FB}^* are typically an order of magnitude smaller than $\Gamma_5^{(*)}$. In this sense, the BD mode is specially interesting since the contribution of the normalization decay to the forward-backward asymmetry is proportional to Γ_{0+}^I in eqs. (30), which in the SM is suppressed by m_ℓ^2 . Therefore, R_{FB} is a very clean observable of the $\bar{B} \rightarrow D\tau^-\bar{\nu}$ decay, at least regarding the possible pollution of the signal from the normalization mode. The same argument does not follow for the BD^* mode because, besides Γ_{0+}^I , A_{FB}^* also receives contributions from decays into transversal D^* which are not suppressed by the light-lepton masses. Thus, the separation of signal from background is crucial to exploit the forward-backward asymmetry in this case.

The angular analysis can also serve to increase the efficiency of the selection of the signal over the background in these decays.³ As an illustration, we show in Fig. 3, the angular distributions of the $\bar{B} \rightarrow D^{(*)}\tau^-(\rightarrow \ell^-\bar{\nu}_\ell\nu_\tau)\bar{\nu}_\tau$ and the $\bar{B} \rightarrow$

³ This has been pointed out recently and independently in ref. [43] for the $\bar{B} \rightarrow P\tau^-\bar{\nu}$ decays, with $P = D, \pi$.

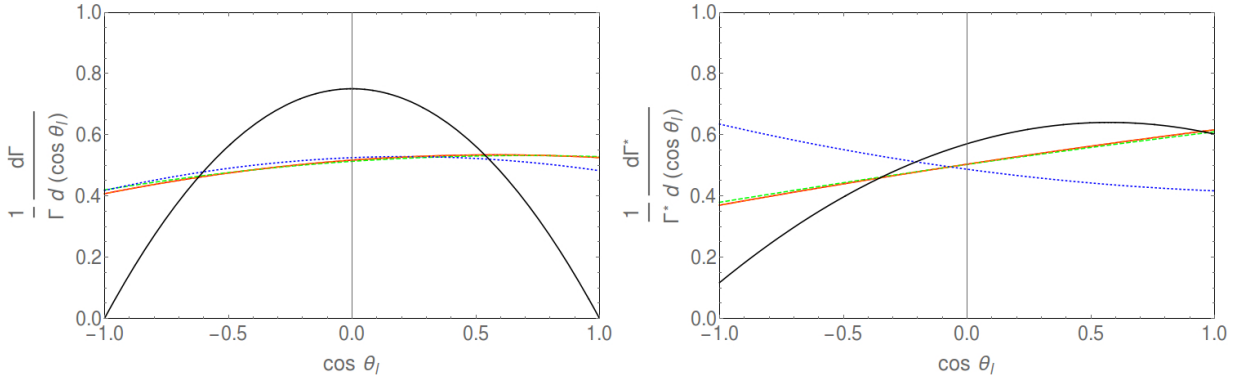


FIG. 3: Angular distribution for the $\bar{B} \rightarrow D^{(*)}\tau^- (\rightarrow \ell^- \bar{\nu}_\ell \nu_\tau) \bar{\nu}_\tau$ decays, in the SM and in the different benchmarks of NP (same code as in Fig. 2), compared to the one of the normalization mode, $\bar{B} \rightarrow D^{(*)}\ell^- \bar{\nu}_\ell$.

$D^{(*)}\ell^- \bar{\nu}$ decays which are quite different. The shape of the distribution of $\bar{B} \rightarrow D\ell^- \bar{\nu}$ is a consequence of the fact that the only contribution to the rate that is not suppressed by m_ℓ^2 in the SM, enters through Γ_{0-} in eqs. (30, 29) and behaves as $\sim \sin^2 \theta_\ell$. In particular, we see another manifestation of the smallness of the forward-backward asymmetry (A_{FB}^ℓ) in this case. In contrast to this, the angular distribution of the $\bar{B} \rightarrow D\tau^- (\rightarrow \ell^- \bar{\nu}_\ell \nu_\tau) \bar{\nu}_\tau$ decay is approximately flat with a slight tilt produced by A_{FB} . On the other hand, the sensitivity of the angular distribution to NP is very small because the effect of NP in the total rate and A_{FB} for the scenarios considered here are similar, canceling the ratio. For the BD^* modes, the sizable A_{FB}^{ℓ} , as well as the more complex dependence produced by the contributions to the rates stemming from different polarization states of the D^* , are visible in the plot. In this case, the effects of the tensor NP scenario is sizable and modify the slope of the distribution in the SM.

V. CONCLUSIONS

The discrepancy between $R_{D^{(*)}}$ as measured by three independent experiments and the standard-model predictions represents one of the most intriguing anomalies in flavor observables. In order to determine whether this is truly the manifestation of the long-sought new physics or a misinterpreted background effect, it is crucial to develop new tools to analyze all possible observables in the $B \rightarrow D^{(*)}\tau\bar{\nu}$ decay. A strategy for achieving this consists of the analysis of the $\bar{B} \rightarrow D^{(*)}\tau^- (\rightarrow \ell^- \bar{\nu}_\ell \nu_\tau) \bar{\nu}_\tau$ decay as a function of the experimentally-accessible variables q^2 , E_ℓ and the angle θ_ℓ between the 3-momentum of the final charged-lepton and the recoiling direction of the $D^{(*)}$.

The present work stands as an initial step from the theory side in this direction, providing an analytic formula for the 3-fold 5-body differential decay rate for both the BD and BD^* modes and including general new physics contributions in the framework of effective field theory. Besides the q^2 - and E_ℓ -spectra of the rates, an angular analysis based on θ_ℓ allows to identify new observables independent of the total rates. For instance, the forward-backward asymmetry captures the contribution to the rate odd under $\theta_\ell \rightarrow \pi - \theta_\ell$ which is otherwise invisible integrating over all phase space. We use this to construct new integrated observables that we call $R_{FB}^{(*)}$. These are quite sensitive to the effects of new physics and could provide complementary sources of information to discriminate among different scenarios. In particular, the asymmetry of the BD mode is very clean in the sense that any pollution induced by the $B \rightarrow D\ell\bar{\nu}$ decay is negligible. On the other hand, the asymmetry in the BD^* channel shows a strong sensitivity to tensorial new-physics contributions.

The angular distribution is not only useful to discriminate among different new-physics scenarios but also to increment the efficiency of the selection of the signal over the normalization process. While the dependence on $\cos \theta_\ell$ of the $B \rightarrow D^{(*)}\ell\bar{\nu}$ rates presents sizable curvature, the ones for $\bar{B} \rightarrow D^{(*)}\tau^- (\rightarrow \ell^- \bar{\nu}_\ell \nu_\tau) \bar{\nu}_\tau$ are quite flat, *viz.* Fig. 3.

Our work can be extended to analyze the full kinematic dependence of the rate, for example by looking at the variation of the angular coefficients $I_i(q^2, E_\ell)$ with the lepton energy and transferred momentum, or converting the formulae to kinematic variables better suited for a given experiment. One could also straightforwardly implement the decay of the D^* in our 5-body formula to obtain the full 6-body differential decay rate. This introduces two new measurable angles that would lead to a string of new angular observables. Finally, our analytic formulae could help to improve the efficiency of the experimental analyses of the data.

VI. ACKNOWLEDGMENTS

We are especially grateful to Karol Adamczyk and Maria Rozanska for calling our attention to a missing contribution in the first version of this preprint. We also would like to thank Marzia Bordone, Ulrik Egede, Ben Grinstein, Gino Isidori, Zoltan Ligeti, Thomas Kuhr, Aneesh Manohar, Mitesh Patel, Vladimir Pascalutsa, Sascha Turczyk and Danny van Dyk and for useful discussions. This work was supported in part by DOE grant de-sc0009919. JMC has received funding from the People Programme (Marie Curie Actions) of the European Union's Seventh Framework Programme (FP7/2007-2013) under REA grant agreement n PIOF-GA-2012-330458. RA thanks the Theory Department at CERN for hospitality during the completion of this work.

Appendix A: Analytic formulas for the angular coefficients

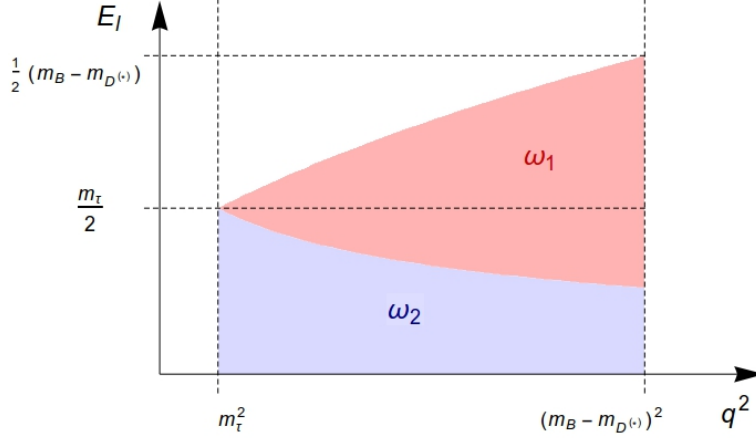


FIG. 4: Phase-space regions of the $I_i(q^2, E_\ell)$ angular coefficients.

The $I_i(q^2, E_\ell)$ angular coefficients are piecewise functions with different expressions for the two different regions of phase space, ω_1 and ω_2 , as described in Sec. III and illustrated in Fig. 4. These functions are best presented via the introduction of dimensionless variables

$$x^2 = \frac{q^2}{m_\tau^2}, \quad y = \frac{E_\ell}{m_\tau}, \quad (\text{A1})$$

and introducing the coefficients of the different powers of $\cos \theta_\tau$ in eq. (29),

$$\begin{aligned} \Gamma_-^{(0)} &= \Gamma_{+-} + \Gamma_{--} + 2\Gamma_{0-}, & \Gamma_+^{(0)} &= 2\Gamma_{0+}^t + \Gamma_{++} + \Gamma_{-+}, \\ \Gamma_-^{(1)} &= 2\Gamma_{--} - 2\Gamma_{+-}, & \Gamma_+^{(1)} &= 2\Gamma_{0+}^I, \\ \Gamma_-^{(2)} &= \Gamma_{+-} + \Gamma_{--} - 2\Gamma_{0-}, & \Gamma_+^{(2)} &= 2\Gamma_{0+}^0 - \Gamma_{++} - \Gamma_{-+}, \end{aligned} \quad (\text{A2})$$

or in eq. (31):

$$\mathcal{I}^{(0)} = 2\text{Re} [2\mathcal{I}_0^I + \mathcal{I}_+ + \mathcal{I}_-], \quad (\text{A3})$$

$$\mathcal{I}^{(1)} = 2\text{Re} [2\mathcal{I}_0 + \mathcal{I}_- - \mathcal{I}_+]. \quad (\text{A4})$$

For the region ω_1 we have,

$$I_0 = \frac{(3x^2 - 2)(x + 4y)(x - 2y)^2}{6x^2(x^2 - 1)^2 y^2} \Gamma_+^{(0)} + \frac{(2x^4 - 3x^2 - 16xy^3 + 12y^2)}{6x(x^2 - 1)^2 y^2} \Gamma_-^{(0)} \\ + \frac{(20x^5 y + x^4(40y^2 - 6) + 16x^3 y(5y^2 - 4) + x^2(15 - 72y^2) - 4xy(8y^2 - 5) + 20y^2)(x - 2y)^2}{120x(x^2 - 1)^4 y^4} \Gamma_-^{(2)} \\ + \frac{(40x^5 y + 5x^4(16y^2 - 3) - 50x^3 y + x^2(6 - 80y^2) + 16xy + 24y^2)(x - 2y)^3}{120x^2(x^2 - 1)^4 y^4} \Gamma_+^{(2)} \quad (\text{A5})$$

$$+ \frac{-240x^5 y^4 + 9x^5 + 32(10x^4 - 5x^2 + 1)y^5 - 30(x^2 + 1)x^4 y + 20(x^4 + 4x^2 + 1)x^3 y^2}{120x(x^2 - 1)^4 y^4} \mathcal{I}^{(1)}, \quad (\text{A6})$$

$$I_1 = \frac{(-2x^4 + x^2 + 4(3x^4 - 3x^2 + 1)y^2 + (3x^4 - 5x^2 + 2)xy)(x - 2y)^2}{6x^2(x^2 - 1)^3 y^3} \Gamma_+^{(1)} \\ + \frac{(2x^6 y - x^5 - 3x^4 y + x^3(2 - 16y^4) + x^2 y(20y^2 - 3) - 4y^3)}{6x(x^2 - 1)^3 y^3} \Gamma_-^{(1)} \quad (\text{A7})$$

$$- \frac{(x - 2y)^2(2x^3 y + x^2(8y^2 - 1) - 2xy - 4y^2)}{6x(x^2 - 1)^3 y^3} \mathcal{I}^{(0)}, \quad (\text{A8})$$

$$I_2 = \frac{1}{120(x^2 - 1)^4 y^4} \left[720x^3 y^4 - 64(5(x^4 + x^2) - 1)y^5 - 60x^2(x^4 - 2x^2 - 2)y + 9x^3(2x^2 - 5) \right. \\ \left. + 20x(2x^6 - x^4 - 16x^2 - 3)y^2 \right] \Gamma_-^{(2)} + \frac{1}{120x^2(x^2 - 1)^4 y^4} \left[-720x^7 y^4 + 9(5x^2 - 2)x^5 \right. \\ \left. - 60(2(x^4 + x^2) - 1)x^4 y + 64(5(3x^6 - 2x^4 + x^2) - 1)y^5 + 20(3x^6 + 16x^4 + x^2 - 2)x^3 y^2 \right] \Gamma_+^{(2)} \quad (\text{A9})$$

$$+ \frac{240x^5 y^4 - 9x^5 - 32(10x^4 - 5x^2 + 1)y^5 + 30(x^2 + 1)x^4 y - 20(x^4 + 4x^2 + 1)x^3 y^2}{40x(x^2 - 1)^4 y^4} \mathcal{I}^{(1)}, \quad (\text{A10})$$

and for the region ω_2 ,

$$I_0 = -\frac{2(2x^2 + 1)(4xy - 3)}{3x} \Gamma_-^{(0)} + \frac{2(x^2 + 2)(3x - 4y)}{3x^2} \Gamma_+^{(0)} \\ + \frac{2}{15} \left(-12x^2 y + 10x + \frac{5}{x} - 8y \right) \Gamma_-^{(2)} + \frac{(10x(x^2 + 2) - 8(2x^2 + 3)y)}{15x^2} \Gamma_+^{(2)} - \frac{4(x^2 - 1)y}{15x} \mathcal{I}^{(1)}, \quad (\text{A11})$$

$$I_1 = \frac{(8x^3 y - 4x^2 + 2)}{3x} \Gamma_-^{(1)} - \frac{2(x^3 - 2x + 4y)}{3x^2} \Gamma_+^{(1)} + \frac{4}{3} \left(-2xy - \frac{2y}{x} + 1 \right) \mathcal{I}^{(0)}, \quad (\text{A12})$$

$$I_2 = \frac{8(x^2 - 1)y}{15x^2} \Gamma_+^{(2)} - \frac{8}{15}(x^2 - 1)y \Gamma_-^{(2)} + \frac{4(x^2 - 1)y}{5x} \mathcal{I}^{(1)}. \quad (\text{A13})$$

-
- [1] J. P. Lees et al. (BaBar), Phys. Rev. Lett. **109**, 101802 (2012), 1205.5442.
[2] J. P. Lees et al. (BaBar), Phys. Rev. **D88**, 072012 (2013), 1303.0571.
[3] M. Huschle et al. (Belle), Phys. Rev. **D92**, 072014 (2015), 1507.03233.
[4] R. Aaij et al. (LHCb), Phys. Rev. Lett. **115**, 111803 (2015), [Addendum: Phys. Rev. Lett.115,no.15,159901(2015)], 1506.08614.
[5] E. de Rafael and J. Taron, Phys. Rev. **D50**, 373 (1994), hep-ph/9306214.
[6] C. G. Boyd, B. Grinstein, and R. F. Lebed, Nucl. Phys. **B461**, 493 (1996), hep-ph/9508211.
[7] I. Caprini, L. Lellouch, and M. Neubert, Nucl. Phys. **B530**, 153 (1998), hep-ph/9712417.

- [8] Y. Amhis et al. (Heavy Flavor Averaging Group (HFAG)) (2014), 1412.7515.
- [9] D. Becirevic, N. Kosnik, and A. Tayduganov, Phys.Lett. **B716**, 208 (2012), 1206.4977.
- [10] J. A. Bailey et al. (MILC), Phys. Rev. **D92**, 034506 (2015), 1503.07237.
- [11] H. Na, C. M. Bouchard, G. P. Lepage, C. Monahan, and J. Shigemitsu (HPQCD), Phys. Rev. **D92**, 054510 (2015), 1505.03925.
- [12] D. Du, A. X. El-Khadra, S. Gottlieb, A. S. Kronfeld, J. Laiho, E. Lunghi, R. S. Van de Water, and R. Zhou, Phys. Rev. **D93**, 034005 (2016), 1510.02349.
- [13] S. Fajfer, J. F. Kamenik, and I. Nisandzic, Phys.Rev. **D85**, 094025 (2012), 1203.2654.
- [14] A. Crivellin, C. Greub, and A. Kokulu, Phys. Rev. **D86**, 054014 (2012), 1206.2634.
- [15] A. Celis, M. Jung, X.-Q. Li, and A. Pich, JHEP **1301**, 054 (2013), 1210.8443.
- [16] A. Datta, M. Duraisamy, and D. Ghosh, Phys. Rev. **D86**, 034027 (2012), 1206.3760.
- [17] M. Tanaka and R. Watanabe, Phys. Rev. **D87**, 034028 (2013), 1212.1878.
- [18] P. Ko, Y. Omura, and C. Yu, JHEP **03**, 151 (2013), 1212.4607.
- [19] Y. Sakaki, M. Tanaka, A. Tayduganov, and R. Watanabe, Phys.Rev. **D88**, 094012 (2013), 1309.0301.
- [20] M. Duraisamy and A. Datta, JHEP **09**, 059 (2013), 1302.7031.
- [21] P. Biancofiore, P. Colangelo, and F. De Fazio, Phys. Rev. **D87**, 074010 (2013), 1302.1042.
- [22] Y. Sakaki, M. Tanaka, A. Tayduganov, and R. Watanabe, Phys. Rev. **D91**, 114028 (2015), 1412.3761.
- [23] R. Alonso, B. Grinstein, and J. M. Camalich, JHEP **10**, 184 (2015), 1505.05164.
- [24] M. Freytsis, Z. Ligeti, and J. T. Ruderman, Phys. Rev. **D92**, 054018 (2015), 1506.08896.
- [25] R. Barbieri, G. Isidori, A. Pattori, and F. Senia, Eur. Phys. J. **C76**, 67 (2016), 1512.01560.
- [26] A. Crivellin, J. Heeck, and P. Stoffer, Phys. Rev. Lett. **116**, 081801 (2016), 1507.07567.
- [27] L. Calibbi, A. Crivellin, and T. Ota, Phys. Rev. Lett. **115**, 181801 (2015), 1506.02661.
- [28] S. Fajfer and N. Košnik (2015), 1511.06024.
- [29] S. Bhattacharya, S. Nandi, and S. K. Patra, Phys. Rev. **D93**, 034011 (2016), 1509.07259.
- [30] M. Bauer and M. Neubert (2015), 1511.01900.
- [31] U. Nierste, S. Trine, and S. Westhoff, Phys. Rev. **D78**, 015006 (2008), 0801.4938.
- [32] M. Tanaka and R. Watanabe, Phys. Rev. **D82**, 034027 (2010), 1005.4306.
- [33] K. Hagiwara, M. M. Nojiri, and Y. Sakaki, Phys. Rev. **D89**, 094009 (2014), 1403.5892.
- [34] A. J. Bevan et al. (Belle, BaBar), Eur. Phys. J. **C74**, 3026 (2014), 1406.6311.
- [35] V. Cirigliano, J. Jenkins, and M. Gonzalez-Alonso, Nucl.Phys. **B830**, 95 (2010), 0908.1754.
- [36] A. Sirlin, Nucl. Phys. **B196**, 83 (1982).
- [37] W. Buchmuller and D. Wyler, Nucl. Phys. **B268**, 621 (1986).
- [38] D. Becirevic, S. Fajfer, I. Nisandzic, and A. Tayduganov (2016), 1602.03030.
- [39] J. A. Bailey et al. (Fermilab Lattice, MILC), Phys. Rev. **D89**, 114504 (2014), 1403.0635.
- [40] M. Tanaka, Z. Phys. **C67**, 321 (1995), hep-ph/9411405.
- [41] K. A. Olive et al. (Particle Data Group), Chin. Phys. **C38**, 090001 (2014).
- [42] D. A. Dicus, E. C. G. Sudarshan, and X. Tata, Phys. Lett. **B154**, 79 (1985).
- [43] M. Bordone, G. Isidori, and D. van Dyk (2016), 1602.06143.